International Journal of Pharmaceutics 409 (2011) 46–56

Contents lists available at ScienceDirect

International Journal of Pharmaceutics

journal homepage: www.elsevier.com/locate/ijpharm

Synthesis and DNA transfection properties of new head group modified malonic acid diamides

Christian Wölk[a], Martin Heinze[a,1], Patrick Kreideweiß[a], Matthias Dittrich[b], Gerald Brezesinski[b], Andreas Langner[a], Bodo Dobner[a,*]

[a] Institute of Pharmacy, Department of Biochemical Pharmacy, Martin-Luther-University Halle-Wittenberg, Wolfgang-Langenbeck-Strasse 4, 06120 Halle (Saale), Germany
[b] Max Planck Institute of Colloids and Interfaces, Science Park Potsdam-Golm, Am Muehlenberg 1, 14476 Potsdam, Germany

ARTICLE INFO

Article history:
Received 4 November 2010
Received in revised form 14 February 2011
Accepted 17 February 2011
Available online 25 February 2011

Keywords:
Cationic lipids
Malonic acid diamides
Synthetic methods
Liposomes
Lipoplexes
Non-viral gene transfer

ABSTRACT

Malonic acid diamides with two long hydrophobic alkyl chains and a basic polar head group as a new class of non-viral gene transferring compounds have shown high transfection efficiency and moderate toxicity. Based on the results obtained with saturated and unsaturated alkyl residues new derivatives with a more complex head group structure have been synthesized. For this purpose, cationic respectively basic groups were introduced by one or two lysine residues bound via tris(aminoethyl)amine spacer to the malonic acid diamide backbone. By studying *in vitro* gene delivery an increase of transfection efficacy was observed when using lipids with at least one unsaturated alkyl chain. This leads to cationic lipids exhibiting comparable or even higher transfection efficacies compared to the commercially available transfection agents LipofectAmine™ and SuperFect™. Phase transitions and phase structures of selected compounds have been analyzed and discussed in terms of transfection abilities. Particle size and zeta potential of liposomes and lipoplexes were also determined.

1. Introduction

Gene therapy is a promising method not only for the treatment of inherited diseases such as cystic fibrosis (Hyde et al., 2000; Noone et al., 2000) but also for acquired diseases like cancer, AIDS, and diabetes (Nazari and Jashi, 2009; Young et al., 2007; Zhang et al., 2009). This therapy is also a great challenge to all researchers dealing with the problem of back-door recruitment of genetic material into cells and organisms. In general, gene delivery systems are mainly based on either viral or non-viral vectors (El-Aneed, 2004). Although the viral gene delivery systems have a higher efficiency in gene transfer than the non-viral ones, they are still associated with problems like immunogenic potential, restrictions with regard to the size of delivered genetic material, difficult production, and oncogenic potential (Kay et al., 2001; Seow and Wood, 2009). Therefore, parallel to further experiments with certain viruses the molecular design and synthesis of new non-viral vectors was pushed and has now reached a remarkable advance both in quantity and quality (Mintzer and Simanek, 2009). Especially the synthesis of cationic lipids has generated new and interesting substances (Bhattacharya and Bajaj, 2009). Nevertheless, the results achieved with the new compounds transfecting polynucleotides into cells are not yet satisfactorily, mainly because of the low transfection efficiency compared to viral vectors. Therefore, one of primary tasks in the cationic lipid mediated gene delivery consists in the design and synthesis of new vectors, based on structural investigations of the lipoplex (cationic lipid–DNA complex) morphology, to further improve the transfection efficacy (Ma et al., 2007). In general, the cationic lipids used for gene transfer have the same schematic structure consisting of three respectively four molecular parts: the hydrophobic chains which are assumed to be responsible for the formation of liposomes, in some lipids a backbone like glycerol, the spacer, and the cationic head group. High efficiency in gene delivery relies on an optimized interplay between these parts. Furthermore, the co-lipid as an additional component plays an important role to achieve high transfection efficacy (Ma et al., 2007; Zidovska et al., 2009).

Abbreviations: Boc-Lys(Boc)-OSu, N_{α},N_{ε}-di-boc-L-lysine-*N*-hydroxysuccinimide ester; BOP, (benzotriazol-1-yloxy)-tris(dimethylamino)-phosphoniumhexafluorophosphate; DOPE, 1,2-dioleoyl-*sn*-glycero-3-phosphoethanolamine; DSC, differential scanning calorimetry; EEDQ, 2-ethoxy-1-ethoxycarbonyl-1,2-dihydrochinoline; FBS, fetal bovine serum; MTT, 3-(4,5-dimethylthiazol-2-yl)-2,5-diphenyltetrazolium bromide; N/P ratio, protonable nitrogen of cytofectines/phosphate groups of DNA - ratio; ONPG, *O*-nitrophenyl-β-galactopyranoside; PCS, photon correlation spectroscopy; PyBOP®, (benzotriazol-1-yloxy)-tripyrrolidino-phosphoniumhexafluorophosphate; WAXS, wide angle X-ray scattering.

* Corresponding author. Tel.: +49 345 55 25120; fax: +49 345 55 27018.
E-mail address: bodo.dobner@pharmazie.uni-halle.de (B. Dobner).
[1] Present address: Universitätsklinikum Halle (Saale), Universitätsapotheke, Ernst-Grube-Straße 40, 06092 Halle (Saale), Germany.

0378-5173/$ – see front matter © 2011 Elsevier B.V. All rights reserved.
doi:10.1016/j.ijpharm.2011.02.022

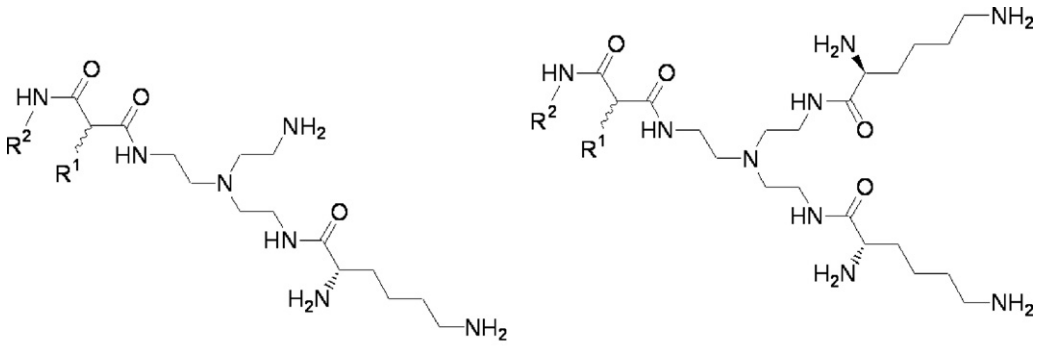

lipid 1 (8a): R^1= R^2= hexadecyl
lipid 2 (8b): R^1= hexadecyl R^2= oleyl
lipid 3 (8c): R^1= R^2= oleyl
lipid 4 (9a): R^1= R^2= hexadecyl
lipid 5 (9b): R^1= hexadecyl R^2= oleyl
lipid 6 (9c): R^1= R^2= oleyl

Fig. 1. Structures and abbreviations of the six novel cationic lipids containing malonic acid diamide backbone.

Recently, we have reported on a new class of cationic lipids based on a malonic acid diamide structure as the backbone with two hydrophobic chains attached (Heinze et al., 2010). The amide bonds, which connect one hydrophobic chain and the spacer as well as the polar head group with the backbone, ensure biodegradability which is necessary for low toxicity of the compounds (Lv et al., 2006). Besides, amide bonds show higher stability with regard to hydrolysis than ester bonds. Furthermore, a positive effect may result from the planar geometry of the amide bonds which in combination with the formation of a hydrogen bond network promotes lamellar phases of the lipoplexes. Hence, we found good serum stability compared to the commercially available transfection reagents. Also the synthesis used is a practicable method using easily accessible materials. Starting from simple alkyl malonic acid monoesters, the second hydrophobic chain, which is necessary for effective transfection, was introduced by malonic acid amide formation with long chain alkyl amines like hexadecylamine or oleylamine. The cationic head group is formed via ethylene diamine or tris(aminoethyl)amine groups or the amino acid lysine using ethylene diamine as spacer receiving an oligoamide structure. These new compounds have shown transfection efficiencies comparable or even higher than LipofectAmine™ or SuperFect™ depending on the saturation degree of the hydrophobic chains and on the size of the head group. As an extension of this work, we report here about the synthesis and transfection characteristics of six new multivalent cationic lipids with malonic acid diamide backbone and an enlarged head group by coupling with one or two lysine molecules using tris(aminoethyl)amine as spacer (Fig. 1).

In addition, we have varied the alkyl chains by using different combinations of hexadecyl and oleyl chains with the aim to investigate structure–activity relationships. Lysine as a basic proteinogenic amino acid enables the introduction of protonable amino groups in the head group region of the lipids. Furthermore, lysine has the ability to complex DNA as an element of histones and poly-L-lysine (Luger et al., 1997; Park et al., 2006). The new compounds were tested in cell cultures with regard to transfection efficacy and toxicity properties. Furthermore, the cationic liposomes and lipoplexes have been investigated with regard to their size and surface charge by PCS[2] and zeta potential measurements. Selected lipids have been also investigated by DSC[2] and WAXS[2] experiments to determine phase transitions and phase structures. The physical–chemical characterization has been performed with the aim to obtain structure–function correlations of the used lipid mixtures.

2. Material and methods

2.1. General procedures and materials

All materials and reagents were purchased from Sigma–Aldrich Co. Ltd. unless stated otherwise. All solvents were analytically pure and dried before use. Thin layer chromatography was carried out on aluminum sheets coated with silica gel 60 F254 (Merck, Darmstadt, Germany) and visualized with bromothymol blue. For column chromatography under normal pressure silica gel 60 (0.036–0.200 mm) was used. Mass spectrometry analyses were performed with a Finnigan MAT 710C (Thermoseparation Products, San Jose, USA) for the ESI-MS spectra, and with a LTQ (linear ion trap)-Orbitrap XL hybrid mass spectrometer (Thermo Fisher Scientific, Bremen, Germany) for the HR-MS (high resolution mass spectrometry) spectra. ^{1}H NMR and ^{13}C NMR spectra were recorded on a Varian Gemini 2000 and a Varian Inova 500. Elemental analyses were performed with a CHNS-932 (Leco-corporation, St Joseph, Michigan, USA). SuperFect™ and plasmid isolation kit were purchased from QIAGEN (QIAGEN, Hilden, Germany). p-CMV-SPORT-β-Gal plasmid and LipofectAmine™ reagent were purchased from Invitrogen Life Technologies (Germany). A549 cells were purchased from German Collection of Microoganisms and Cell Cultures (DSMZ GmbH, Germany), and LLC PK1 cells (ATCC CL-11101) from the American Type Culture Collection (ATCC, USA). Fetal bovine serum, cell culture media, and phosphate buffered saline were obtained from PAA Laboratories (PAA Laboratories GmbH, Germany). Antibiotics and MTT[2] were purchased from Sigma (Sigma–Aldrich, Germany). DOPE[2] was purchased from Fluka (Fluka Chemie AG, Switzerland), and cholesterol from Roth (Carl Roth GmbH, Germany).

2.2. Synthesis of the compounds

The synthesis of **1a,b**; **2a,b**; **3a–c** and **4a–c** is already described (Heinze et al., 2010).

2.2.1. Coupling of lipophilic malonic acid monoamides with tris(aminoethyl)amine

Reaction of compound 4a–c with tris(aminoethyl)amine to 5a–c:

General procedure: A solution of the acid **4a**, **4b** or **4c** (1 mmol) and PyBOP®[2] (1 mmol, 520 mg) in CH_2Cl_2 (40 mL) was added dropwise to a mixture of tris(aminoethyl)amine (20 mmol, 2.93 g) and tri-

ethylamine (1.5 mmol, 152 mg) under stirring. The mixture was stirred at room temperature for 4 h. Then the solution was filtered, washed with water and brine, dried over sodium sulfate, filtered, and the solvent was evaporated. The crude compound **5a–c** was purified by column chromatography using silica gel 60 and $CHCl_3$/methanol/NH_3 with gradient technique.

N-{2-[*N*,*N*-Bis(2-aminoethyl)amino]ethyl}-*N*′,2-dihexadecylpropane diamide (**5a**): Yield: 71.2%.
N-{2-[*N*,*N*-Bis(2-aminoethyl)amino]ethyl}-2-hexadecyl-*N*′-[(9*Z*)-octadec-9-enyl]propane diamide (**5b**): Yield: 64.4%.
N-{2-[*N*,*N*-Bis(2-aminoethyl)amino]ethyl}-*N*′,2-[(9*Z*)-octadec-9-enyl]propane diamide (**5c**): Yield: 85.5%.

The experimental data of the compounds **5a–c** are in agreement with the literature (Heinze et al., 2010).

2.2.2. Coupling of malonic acid diamides with one Boc-protected lysine moiety

*2.2.2.1. Reaction **5a–c** to Compounds **6a–c**. General procedure*: Compound **5a**, **5b** or **5c** (1 mmol) and triethylamine (1 mmol, 101 mg) were dissolved in CH_2Cl_2 (20 mL). N_α,N_ε-di-boc-L-lysine-*N*-hydroxysuccinimide ester (0.5 mmol, 220 mg) was given to this solution. The mixture was stirred for 1 h at room temperature. Following the solvent was evaporated. The residue was dissolved in $CHCl_3$ (50 mL), the organic solution was washed with a potassium carbonate solution (15% m/m), dried over sodium sulfate, filtered, and the solvent was evaporated. The crude products **6a–c** were purified by column chromatography using silica gel 60 and $CHCl_3$/methanol/NH_3 with gradient technique.

*2.2.2.2. N-(2-{N-(2-Aminoethyl)-N-[2-(N-{2,6-di[N-(tert.-butoxycarbonyl)amino]-1-oxohexyl}amino)ethyl]amino}ethyl)-N′,2-dihexadecylpropane diamide (**6a**).* Yield: 41.7%; glass-like colorless substance; $C_{57}H_{113}N_7O_7$; *M*: 1008.55 g mol^{-1}; m.p. 47–50 °C; ESI-MS: *m*/*z*: 1009.5 $[M+H]^+$, 1043.2 $[M+Cl]^-$; ^{1}H NMR ($CDCl_3$, 400 MHz, 27 °C) δ (ppm): 0.86 (t, $^3J_{H,H}$ = 6.6 Hz, 6H, 2[–CH_2CH_3]), 1.08–1.80 (m, 82H, [–$(CH_2)_{15}CH_3$] [–$CH_2(CH_2)_{14}CH_3$] 2[–$C(CH_3)_3$] [–$(CH_2)_3CH_2$NHBoc]), 2.54–2.95 (m, 8H, [–NHCH$_2$CH$_2$N(CH$_2$CH$_2$NH–)(CH$_2$CH$_2$NH$_2$)]), 3.09–3.72 (m, 9H, 3[–CONHCH$_2$–] [–CH$_2$NHBoc] [–COCHCO–]), 4.38–4.39 (m, 1H, [–COCHNHBoc–]), 4.69–4.76/6.47–6.51/7.99–8.06/8.43–8.56/9.09–9.19 (5 × m, 5H, 2[–NHBoc] 3[–NHCO–]); Anal. calcd. for $C_{57}H_{113}N_7O_7 \cdot 2H_2O$: C, 65.54; H, 11.29; N, 9.39; found: C, 65.65; H, 11.16; N, 9.35.

*2.2.2.3. N-(2-{N-(2-Aminoethyl)-N-[2-(N-{2,6-di[N-(tert.-butoxycarbonyl)amino]-1-oxohexyl}amino)ethyl]amino}ethyl)-2-hexadecyl-N′-[(9Z)-octadec-9-enyl]propane diamide (**6b**).* Yield: 38.5%; glass-like colorless substance; $C_{59}H_{115}N_7O_7$; *M*: 1034.58 g mol^{-1}; m.p. 36–39 °C; ESI-MS: *m*/*z*: 1035.5 $[M+H]^+$, 1069.3 $[M+Cl]^-$; ^{1}H NMR ($CDCl_3$, 500 MHz, 27 °C) δ (ppm): 0.86 (t, $^3J_{H,H}$ = 6.9 Hz, 6H, 2[–CH_2CH_3]), 1.22–1.82 (m, 78H, [–$(CH_2)_{15}CH_3$] [–$(CH_2)_6CH_2(CH)_2CH_2(CH_2)_6CH_3$] 2[–$C(CH_3)_3$] [–$(CH_2)_3CH_2$NHBoc]), 1.93–1.99 (m, 4H, [–$CH_2(CH)_2CH_2$–]), 2.44–2.94 (m, 8H, [–NHCH$_2$CH$_2$N(CH$_2$CH$_2$NH–)(CH$_2$CH$_2$NH$_2$)]), 3.08–3.75 (m, 9H, 3[–CONHCH$_2$–] [–CH$_2$NHBoc] [–COCHCO–]), 4.39–4.41 (m, 1H, [–COCHNHBoc–]), 5.31–5.36 (m, 2H, [–CH=CH–]), 4.71–4.79/6.46–6.55/7.99–8.04/8.29–8.52/9.07–9.16 (5 × m, 5H, 2[–NHBoc] 3[–NHCO–]); Anal. calcd. for $C_{59}H_{115}N_7O_7 \cdot 1.5H_2O$: C, 66.75; H, 11.20; N, 9.24; found: C, 66.67; H, 11.02; N, 9.10.

*2.2.2.4. N-(2-{N-(2-Aminoethyl)-N-[2-(N-{2,6-di[N-(tert.-butoxycarbonyl)amino]-1-oxohexyl}amino)ethyl]amino}ethyl)-N′,2-di[(9Z)-octadec-9-enyl]propane diamide (**6c**).* Yield: 36.5%; glass-like colorless substance; $C_{61}H_{117}N_7O_7$; *M*: 1060.64 g mol^{-1}; m.p. 42–44 °C; ESI-MS: *m*/*z*: 1060.6 $[M+H]^+$, 1094.5 $[M+Cl]^-$; ^{1}H NMR ($CDCl_3$, 400 MHz, 27 °C) δ (ppm): 0.86 (t, $^3J_{H,H}$ = 6.3 Hz, 6H, 2[–CH_2CH_3]), 1.24–1.82 (m, 74H, [–$(CH_2)_7CH_2(CH)_2CH_2(CH_2)_6CH_3$] [–$(CH_2)_6CH_2(CH)_2CH_2(CH_2)_6CH_3$] 2[–$C(CH_3)_3$] [–$(CH_2)_3CH_2$NHBoc]), 1.96–1.99 (m, 8H, 2[–$CH_2(CH)_2CH_2$–]), 2.47–2.82 (m, 8H, [–NHCH$_2$CH$_2$N(CH$_2$CH$_2$NH–)(CH$_2$CH$_2$NH$_2$)]), 3.08–3.44 (m, 9H, 3[–CONHCH$_2$–] [–CH$_2$NHBoc] [–COCHCO–]), 4.20–4.29 (m, 1H, [–COCHNHBoc–]), 5.30–5.36 (m, 4H, 2[–CH=CH–]), 4.77–4.84/6.76–6.79/7.97–7.99/8.19–8.22/9.02–9.17 (5 × m, 5H, 2[–NHBoc] 3[–NHCO–]); Anal. calcd. for $C_{61}H_{117}N_7O_7$: C, 69.08; H, 11.12; N, 9.24; found: C, 69.27; H, 11.21; N, 9.46.

2.2.3. Coupling of malonic acid diamides with two Boc-protected lysine moieties

*2.2.3.1. Reaction **5a–c** to compounds **7a–c**. Procedure 1*: The reaction was performed as described for the synthesis of **6a–c** with the difference that 1 mmol of compound **5a** was treated with 2 mmol (887 mg) of N_α,N_ε-di-boc-L-lysine-*N*-hydroxysuccinimide ester.

Procedure 2: The reaction was performed as described for the synthesis of **6a–c** with the difference that 1 mmol of compound **5b** or **5c** was treated with 1.5 mmol (665 mg) of N_α,N_ε-di-boc-L-lysine-*N*-hydroxysuccinimide ester.

*2.2.3.2. N-(2-{N,N-Bis[2-(N-{2,6-di[N-(tert.-butoxycarbonyl)amino]-1-oxohexyl}amino)ethyl]amino}ethyl)-N′,2-dihexadecylpropane diamide (**7a**).* Yield: 92% (procedure 1); glass-like colorless substance; $C_{73}H_{141}N_9O_{12}$; *M*: 1336.95 g mol^{-1}; m.p. 44–46 °C; ESI-MS: *m*/*z*:1338.0 $[M+H]^+$, 1371.3 $[M+Cl]^-$; ^{1}H NMR ($CDCl_3$, 400 MHz, 27 °C) δ (ppm): 0.86 (t, $^3J_{H,H}$ = 6.7 Hz, 6H, 2[–CH_2CH_3]), 1.23–1.77 (m, 106H, [–$(CH_2)_{15}CH_3$] [–$(CH_2)_{14}CH_3$] 4[–$C(CH_3)_3$] 2[–$(CH_2)_3CH_2$NHBoc]), 2.46–2.52 (m, 6H, [–NHCH$_2$CH$_2$N(CH$_2$CH$_2$NH–)$_2$]), 3.08–3.47 (m, 13H, 4[–CONHCH$_2$–] 2[–CH$_2$NHBoc] [–COCHCO–]), 4.21–4.30 (m, 2H, 2[–COCHNHBoc–]), 4.76–4.84/5.61–5.63/6.95–6.99/7.41–7.46/7.63–7.66/7.82–7.92 (6 × m, 8H, 4[–NHBoc] 4[–NHCO–]); Anal. calcd. for $C_{73}H_{141}N_9O_{12}$: C, 65.58; H, 10.63; N, 9.43; found: C, 65.76; H, 10.26; N 9.31.

*2.2.3.3. N-(2-{N,N-Bis[2-(N-{2,6-di[N-(tert.-butoxycarbonyl)amino]-1-oxohexyl}amino)ethyl]amino}ethyl)-2-hexadecyl-N′-[(9Z)-octadec-9-enyl]propane diamide (**7b**).* Yield: 70.2% (procedure 2); glass-like substance; $C_{75}H_{143}N_9O_{12}$; *M*: 1362.99 g mol^{-1}; m.p. 35–37 °C; ESI-MS: *m*/*z*: 1363.8 $[M+H]^+$, 1397.2 $[M+Cl]^-$; ^{1}H NMR ($CDCl_3$, 400 MHz, 27 °C) δ (ppm): 0.86 (t, $^3J_{H,H}$ = 6.7 Hz, 6H, 2[–CH_2CH_3]), 1.24–1.77 (m, 102H, [–$(CH_2)_{15}CH_3$] [–$(CH_2)_6CH_2(CH)_2CH_2(CH_2)_6CH_3$] 4[–$C(CH_3)_3$] 2[–$(CH_2)_3CH_2$NHBoc]), 1.94–1.99 (m, 4H, [–$CH_2(CH)_2CH_2$–]), 2.45–2.57 (m, 6H, [–NHCH$_2$CH$_2$N(CH$_2$CH$_2$NH–)$_2$]), 2.91–3.51 (m, 13H, 4[–CONHCH$_2$–] 2[–CH$_2$NHBoc] [–COCHCO–]), 4.22–4.27 (m, 2H, 2[–COCHNHBoc–]), 5.32–5.36 (m, 2H, [–CH=CH–]), 4.76–4.84/5.60–5.62/6.94–6.98/7.42–7.47/7.62–7.66/7.84–7.91 (6 × m, 8H, 4[–NHBoc] 4[–NHCO–]); Anal. calcd. for $C_{75}H_{143}N_9O_{12}$: C, 66.09; H, 10.57; N, 9.25; found: C, 66.15; H, 10.91; N, 9.48.

*2.2.3.4. N-(2-{N,N-Bis[2-(N-{2,6-di[N-(tert.-butoxycarbonyl)amino]-1-oxohexyl}amino)ethyl]amino}ethyl)-N′,2-di[(9Z)-octadec-9-enyl]propane diamide (**7c**).* Yield: 61% (procedure 2); glass-like colorless substance; $C_{77}H_{145}N_9O_{12}$; *M*: 1389.03 g mol^{-1}; m.p. 61–62 °C; ESI-MS: *m*/*z*: 1389.5 $[M+H]^+$, 1424.8 $[M+Cl]^-$; ^{1}H NMR ($CDCl_3$, 400 MHz, 27 °C) δ (ppm): 0.86 (t, $^3J_{H,H}$ = 6.8 Hz, 6H, 2[–CH_2CH_3]), 1.24–1.75 (m, 98H, [–$(CH_2)_7CH_2(CH)_2CH_2(CH_2)_6CH_3$] [–$(CH_2)_6CH_2(CH)_2CH_2(CH_2)_6CH_3$] 4[–$C(CH_3)_3$] 2[–$(CH_2)_3CH_2$NHBoc]), 1.96–1.99 (m, 8H, 2[–$CH_2(CH)_2CH_2$–]), 2.45–2.56 (m, 6H, [–NHCH$_2$CH$_2$N(CH$_2$CH$_2$NH–)$_2$]), 2.91–3.36 (m, 13H, 4[–CONHCH$_2$–] 2[–CH$_2$NHBoc] [–COCHCO–]), 4.22–4.25

(m, 2H, 2[–COC*H*NHBoc–]), 5.27–5.36 (m, 4H, 2[–C*H*=C*H*–]), 4.76–4.84/5.61–5.64/6.95–6.98/7.42–7.47/7.64–7.67/7.83–7.92 (6 × m, 8H, 4[–N*H*Boc] 4[–N*H*CO–]), Anal. calcd. for $C_{77}H_{145}N_9O_{12}$: C, 66.58; H, 10.52; N, 9.08; found: C, 66.61; H, 10.23; N, 9.03.

2.2.4. Deprotection of amino groups

*2.2.4.1. Removal of the Boc group from **6a–c** and **7a–c** to synthesize compounds **8a–c** and **9a–c**. General procedure*: Compound **6a–c** or **7a–c** (1 mmol) was dissolved in CH_2Cl_2 (20 mL). The solution was treated with trifluoro acetic acid (5 mL) under stirring. The mixture was allowed to stir for 5 h, then diluted with $CHCl_3$ (50 mL), and washed with diluted ammonia (3% m/m) until the water layer shows a pH-value above 7. The organic layer was separated, dried over sodium sulfate, filtered, and the solvent was evaporated. The products **8a–c** and **9a–c** were purified by column chromatography using silica gel 60 and $CHCl_3$/methanol/NH_3 with gradient technique.

*2.2.4.2. N-[2-(N-(2-Aminoethyl)-N-{2-[N-(2,6-diamino-1-oxohexyl)amino]ethyl}amino)ethyl]-N′,2-dihexadecylpropane diamide (**8a**).* Yield: 87%; white crystalline substance; $C_{47}H_{97}N_7O_3$; *M*: 808.32 g mol^{-1}; m.p. 74–75 °C; ESI-MS: *m*/*z*: 808.8 $[M+H]^+$, 405.6 $[M+2H]^{2+}$; HR-MS calcd.: 808.7726 $[M+H]^+$, found: 808.7727; ^{1}H NMR ($CDCl_3$, 400 MHz, 27 °C) δ (ppm): 0.85 (t, $^3J_{H,H}$ = 6.7 Hz, 6H, 2[–CH_2CH_3]), 1.22–1.55 (m, 64H, [–(CH_2)$_{15}CH_3$] [–(CH_2)$_{14}CH_3$] [–(CH_2)$_3CH_2NH_2$]), 2.55–2.56 (m, 6H, [–NHCH_2CH_2N(CH_2CH_2NH–)(CH_2CH_2NH_2)]), 2.75 (t, $^3J_{H,H}$ = 6.0 Hz, 4H, 2[–CH_2NH_2]), 3.12–3.41 (m, 8H, 3[–CONHCH_2–] [–COC*H*CO–] [–COC*H*NH_2–]), 7.27–7.38/7.85–7.93/8.16–8.23 (3 × m, 3H, 3[–N*H*CO–]); ^{13}C NMR ($CDCl_3$/CD_3OD, 100 MHz, 27 °C) δ (ppm): 175.64, 171.22, 171.04, 170.96, 54.36, 53.78, 53.60, 53.47, 40.08, 39.35, 39.23, 38.03, 37.31, 37.06, 34.41, 31.57, 29.85, 29.35, 29.30, 29.16, 28.99, 28.90, 27.15, 26.63, 22.31, 13.66.

*2.2.4.3. N-[2-(N-(2-Aminoethyl)-N-{2-[N-(2,6-diamino-1-oxohexyl)amino]ethyl}amino)ethyl]-2-hexadecyl-N′-[(9Z)-octadec-9-enyl]propane diamide (**8b**).* Yield: 97%; white crystalline substance; $C_{49}H_{99}N_7O_3$; *M*: 834.36 g mol^{-1}, m.p. 59–61 °C; ESI-MS: *m*/*z*: 834.8 $[M+H]^+$, 418.4 $[M+2H]^{2+}$; HR-MS calcd.: 832.7882 $[M+H]^+$, found: 832.7886; ^{1}H NMR ($CDCl_3$/CD_3OD, 400 MHz, 27 °C) δ (ppm): 0.78 (t, $^3J_{H,H}$ = 6.4 Hz, 6H, 2[–CH_2CH_3]), 1.15–1.69 (m, 60H, [–(CH_2)$_{15}CH_3$] [–(CH_2)$_6CH_2$(CH)$_2CH_2$(CH_2)$_6CH_3$] [–(CH_2)$_3CH_2NH_2$]), 1.87–1.92 (m, 4H, [–CH_2(CH)$_2$CH_2–]), 2.44–2.48 (m, 6H, [–NHCH_2CH_2N(CH_2CH_2NH–)(CH_2CH_2NH_2)]), 2.64 (t, $^3J_{H,H}$ = 6.0 Hz, 4H, 2[–CH_2NH_2]), 2.89 (s, 6H, 3[–NH_2]), 3.02–3.33 (m, 8H, 3[–CONHCH_2–] [–COC*H*CO–] [–COC*H*NH_2–]), 5.24–5.28 (m, 2H, [–C*H*=C*H*–]), 7.46–7.50/7.90–7.93/8.01–8.12 (3 × m, 3H, 3[–N*H*CO–]); ^{13}C NMR ($CDCl_3$/CD_3OD, 100 MHz, 27 °C) δ (ppm): 175.82, 171.55, 171.29, 129.89, 129.65, 55.43, 54.79, 54.26, 53.98, 53.85, 40.96, 40.94, 39.65, 39.52, 38.69, 37.76, 37.65, 37.36, 37.26, 34.95, 34.90, 32.56, 32.37, 31.89, 31.87, 31.75, 31.57, 31.51, 29.74, 29.68, 29.65, 29.63, 29.49, 29.46, 29.36, 29.32, 29.29, 29.28, 29.15, 27.54, 27.19, 26.95, 22.83, 22.81, 22.65, 14.04.

*2.2.4.4. N-[2-(N-(2-Aminoethyl)-N-{2-[N-(2,6-diamino-1-oxohexyl)amino]ethyl}amino)ethyl]-N′,2-di[(9Z)-octadec-9-enyl]propane diamide (**8c**).* Yield: 91%; white waxy substance; $C_{51}H_{101}N_7O_3$; *M*: 860.39 g mol^{-1}; m.p. 62–65 °C; ESI-MS: *m*/*z*: 861.0 $[M+H]^+$, 431.4 $[M+2H]^{2+}$; HR-MS calcd.: 860.8039 $[M+H]^+$, found: 860.8021; ^{1}H NMR ($CDCl_3$, 400 MHz, 27 °C) δ (ppm): 0.86 (t, $^3J_{H,H}$ = 6.6 Hz, 6H, 2[–CH_2CH_3]), 1.25–1.83 (m, 56H, [–(CH_2)$_7CH_2$(CH)$_2CH_2$(CH_2)$_6CH_3$] [–(CH_2)$_6CH_2$(CH)$_2CH_2$(CH_2)$_6CH_3$] [–(CH_2)$_3CH_2NH_2$]), 1.97–2.00 (m, 8H, 2[–CH_2(CH)$_2$CH_2–]), 2.49–2.57 (m, 6H, [–NHCH_2CH_2N(CH_2CH_2NH–)(CH_2CH_2NH_2)]), 2.70 (t, $^3J_{H,H}$ = 6.4 Hz, 4H, 2[–CH_2NH_2]), 3.05–3.43 (m, 8H, 3[–CONHCH_2] [–COC*H*CO–] [–COC*H*NH_2–]), 5.32–5.36 (m, 4H, 2[–C*H*=C*H*–]), 7.01–7.06/7.82–7.86/8.11–8.16 (3 × m, 3H, 3[–N*H*CO–]); ^{13}C NMR ($CDCl_3$, 100 MHz, 27 °C) δ (ppm): 175.50, 175.43, 171.39, 171.30, 170.99, 129.89, 129.68, 56.18, 55.23, 54.88, 54.51, 53.72, 41.70, 39.57, 39.44, 37.82, 37.20, 37.14, 35.25, 35.13, 32.82, 32.74, 32.67, 32.58, 31.89, 29.76, 29.69, 29.58, 29.54, 29.51, 29.44, 29.39, 29.31, 29.18, 27.68, 27.23, 26.97, 23.12, 22.66, 14.07.

*2.2.4.5. N-[2-(N,N-Bis{2-[N-(2,6-diamino-1-oxohexyl)amino]ethyl}amino)ethyl]-N′,2-dihexadecylpropane diamide (**9a**).* Yield: 89.6%; white crystalline substance; $C_{53}H_{109}N_9O_4$; *M*: 936.49 g mol^{-1}; m.p. 89–91 °C; ESI-MS: *m*/*z*: 937.0 $[M+H]^+$, 469.4 $[M+2H]^{2+}$; HR-MS calcd.: 936.8675 $[M+H]^+$ found: 936.8673; ^{1}H NMR ($CDCl_3$, 400 MHz, 27 °C) δ (ppm): 0.84 (t, $^3J_{H,H}$ = 6.6 Hz, 6H, 2[–CH_2CH_3]), 1.22–1.47 (m, 70H, [–(CH_2)$_{15}CH_3$] [–(CH_2)$_{14}CH_3$] 2[–(CH_2)$_3CH_2NH_2$]), 2.34 (s, 8H, 4[–NH_2]), 2.49–2.53 (m, 6H, [–NHCH_2CH_2N(CH_2CH_2NH–)$_2$]), 2.7 (t, $^3J_{H,H}$ = 6.5 Hz, 4H, 2[–CH_2NH_2]), 3.14–3.41 (m, 11H, 4[–CONHCH_2–] [–COC*H*CO–] 2[–COC*H*NH_2–]), 7.21/7.49/7.69/7.78/7.97/8.05 (6 × t, 4H, 4[–N*H*CO–]); ^{13}C NMR ($CDCl_3$/CD_3OD, 100 MHz, 27 °C) δ (ppm): 175.57, 170.97, 170.82, 54.38, 53.56, 53.43, 53.23, 53.11, 40.41, 39.07, 37.17, 37.01, 34.43, 31.81, 31.42, 31.20, 29.19, 29.14, 29.01, 28.84, 28.76, 27.05, 26.49, 22.41, 22.16, 13.34.

*2.2.4.6. N-[2-(N,N-Bis{2-[N-(2,6-diamino-1-oxohexyl)amino]ethyl}amino)ethyl]-2-hexadecyl-N′-[(9Z)-octadec-9-enyl]propane diamide (**9b**).* Yield: 73%; white crystalline substance; $C_{55}H_{111}N_9O_4$; *M*: 962.53 g mol^{-1}; m.p. 79–81 °C; ESI-MS: *m*/*z*: 963.6 $[M+H]^+$, 482.4 $[M+2H]^{2+}$; HR-MS calcd.: 962.8832 $[M+H]^+$, found: 962.8829; ^{1}H NMR ($CDCl_3$, 500 MHz, 27 °C) δ (ppm): 0.85 (t, $^3J_{H,H}$ = 6.8 Hz, 6H, 2[–CH_2CH_3]), 1.23–1.78 (m, 66H, [–(CH_2)$_{15}CH_3$] [–(CH_2)$_6CH_2$(CH)$_2CH_2$(CH_2)$_6CH_3$] 2[–(CH_2)$_3CH_2NH_2$]), 1.94–1.99 (m, 4H, [–CH_2(CH)$_2$CH_2–]), 2.47–2.55 (m, 6H, [–NHCH_2CH_2N(CH_2CH_2NH–)$_2$]), 2.69 (t, $^3J_{H,H}$ = 6.2 Hz, 4H, 2[–CH_2NH_2]), 3.06–3.44 (m, 11H, 4[–CONHCH_2–] [–COC*H*CO–] 2[–COC*H*NH_2–]), 5.32–5.35 (m, 2H, [–C*H*=C*H*–]), 7.98/7.89/7.72/7.66/7.44/7.11 (6 × t, 4H, 4[–N*H*CO–]); ^{13}C NMR ($CDCl_3$, 125 MHz, 27 °C) δ (ppm): 175.38, 175.14, 171.84, 171.39, 171.14, 170.98, 129.93, 129.70, 55.23, 54.93, 54.70, 54.53, 54.43, 54.31, 53.72, 41.68, 41.62, 39.47, 37.97, 37.88, 37.24, 37.14, 35.38, 35.19, 33.01, 32.91, 32.79, 32.56, 31.87, 31.85, 29.72, 29.66, 29.63, 29.61, 29.47, 29.44, 29.36, 29.31, 29.27, 29.26, 29.14, 29.09, 27.64, 27.17, 26.95, 26.91, 23.09, 23.07, 22.64, 14.06.

*2.2.4.7. N-[2-(N,N-Bis{2-[N-(2,6-diamino-1-oxohexyl)amino]ethyl}amino)ethyl]-N′,2-di[(9Z)-octadec-9-enyl]propane diamide (**9c**).* Yield: 94.6%; white waxy substance; $C_{57}H_{113}N_9O_4$; *M*: 988.57 g mol^{-1}, m.p. 83–85 °C; ESI-MS: *m*/*z*: 988.7 $[M+H]^+$ 495.2 $[M+2H]^{2+}$; HR-MS calcd.: 988.8988 $[M+H]^+$, found: 988.8987; ^{1}H NMR ($CDCl_3$, 400 MHz, 27 °C) δ (ppm): 0.81 (t, $^3J_{H,H}$ = 6.9 Hz, 6H, 2[–CH_2CH_3]), 1.20–1.52 (m, 62H, [–(CH_2)$_7CH_2$(CH)$_2CH_2$(CH_2)$_6CH_3$] [–(CH_2)$_6CH_2$(CH)$_2CH_2$(CH_2)$_6CH_3$] 2[–(CH_2)$_3CH_2NH_2$]), 1.73 (s, 8H, 4[–NH_2]), 1.89–1.94 (m, 8H, 2[–CH_2(CH)$_2$CH_2–]), 2.43–2.58 (m, 6H, [–NHCH_2CH_2N(CH_2CH_2NH–)$_2$]), 2.63 (t, $^3J_{H,H}$ = 6.1 Hz, 4H, 2[–CH_2NH_2]), 3.00–3.35 (m, 11H, 4[–CONHCH_2–] [–COC*H*CO–] 2[–COC*H*NH_2–]), 5.24–5.31 (m, 4H, 2[–C*H*=C*H*–]), 7.13/7.45/7.61/7.66/7.84/7.92 (6 × t, 4H, 4[–N*H*CO–]); ^{13}C NMR ($CDCl_3$, 100 MHz, 27 °C) δ (ppm): 175.36, 175.16, 171.68, 171.26, 171.06, 170.92, 129.91, 129.68, 55.37, 55.35, 55.01, 54.81, 54.59, 54.49, 54.32, 53.82, 41.85, 41.82, 39.55, 38.03, 37.94, 37.38, 37.28, 35.44, 35.29, 33.23, 33.18, 32.96, 32.59, 31.89, 29.80, 29.77, 29.69, 29.59, 29.56, 29.51, 29.45, 29.38, 29.32, 29.29, 29.18, 29.13, 28.97, 27.67, 27.24, 27.01, 26.98, 23.19, 23.17, 22.66, 14.09.

2.3. Protocols for in vitro transfection experiments, viability tests, and physical–chemical characterizations

2.3.1. Preparation of liposomes

A $CHCl_3$/methanol solution (9/1, v/v) of the pure cationic lipid was combined with a $CHCl_3$ solution of DOPE or cholesterol, respectively. The mixtures were dried under reduced pressure to remove the organic solvent, and the dried film was vacuum-desiccated for 3 h. The lipid film was dissolved in distilled water at room temperature to a final concentration of 2 mg mL^{-1}. The film was allowed to swell in a water bath at 40 °C for at least 15 min. Subsequently, the lipid mixtures were vortexed and sonicated to clarity in a bath sonicator. The samples were stored in the refrigerator at 4 °C before experiments.

2.3.2. Preparation of plasmid DNA

p-CMV-SPORT-β-Gal was isolated from *Escherichia coli* DH5a (Invitrogen Life Technologies) using a Quiagen plasmid mega kit (Quiagen) following the manufacturer's instructions (Quiagen handbook). DNA with an OD260/OD280 = 1.94 was used for experiments.

2.3.3. Cell cultures

LLC PK1 cells (porcine kidney epithelial cells) were cultured in 75 cm^2 tissue culture flasks in Medium 199 adjusted to contain 2.2 g L^{-1} sodium bicarbonate, 10% FBS[2], and 0.05 mg mL^{-1} gentamycin at 37 °C and 5% CO_2. The cells were grown confluently and were regularly split twice a week. Only cells that had undergone fewer than 30 passages were used for transfection and MTT experiments. A549 cells (human lung carcinoma cells) were cultured in 75 cm^2 tissue culture flasks in Dulbecco's modified eagle medium (DMEM) adjusted to contain 4.5 g L^{-1} glucose, 10% FBS, and 0.05 mg mL^{-1} gentamycin at 37 °C and 5% CO_2. The cells were grown confluently and were regularly split twice a week. For experiments, only cells in the range of passages 20–60 were used.

2.3.4. Transfection biology

16–24 h before transfection, cells were seeded into a 96 well plate at a density of 8000–10,000 cells/well by usage of LLC PK1 and 18,000–20,000 in the case of A549 cells. Lipoplex mixtures were prepared by combining plasmid DNA (0.1 μg per well, 2.5 μg mL^{-1}) with varying amounts of cationic liposome suspension in the absence or presence of 10% serum in Medium 199 or DMEM. The samples were incubated for 15 min at room temperature (total volume 40 μL/well). The N/P ratios were varied from 1:1 to 4:1 or even higher in cases when the results of experiments foreshadow increasing transfection efficacies at higher charge ratios. During this time, cells were washed once with phosphate buffered saline (PBS). Then the complexes were added to the cells. After 4 h of incubation, 160 μL of Medium 199 or DMEM was added to the cells in a way that the final concentration of FBS reached 10%. The medium was refreshed after 24 h, and the reporter gene activity was estimated after 48 h. Therefore, the cells were washed with PBS and lysed for 15 min in lysis buffer (5 mM Chaps in 50 mM Hepes buffer). The solution was taken out of the wells, reunited in safe-lock tubes (Eppendorf), centrifuged, and stored on ice. It was pipeted again in a 96 well plate and substrate solution (1.33 mg mL^{-1} of ONPG[2], $MgCl_2$ 2 mM, β-mercaptoethanol 100 mM in 0.2 M sodium phosphate pH 7.3) was added and incubated for 30 min at 37 °C. The reaction was stopped with 1 M sodium carbonate. Absorption at 405 nm was converted to β-galactosidase units using a calibration curve constructed with pure commercial β-galactosidase enzyme. Protein concentration was detected with bichinonic acid reaction (Rosenberg, 1996). Absorption at 570 nm was converted by using a calibration curve made of bovine serum albumin. All experiments were carried out sixfold. Every experiment was repeated three to five times on different days. For the experiments in the presence of FBS lipoplexes were incubated with the cells as described above, certainly the concentration of serum was adjusted to 10% from the outset of experiments and kept for 48 h.

2.3.5. Toxicity assay

Cytotoxicity of the lipoplexes was assessed by the MTT reduction assay (Mosmann, 1983). The cytotoxicity assays were performed in 96 well plates by maintaining the same ratio and number of cells and lipoplexes as used in the transfection experiments. MTT was added after refreshing the medium (24 h after addition of lipoplexes to the cells) and incubated for 3 h at 37 °C. Afterward, the cells were lysed with a mixture of 10% sodium dodecyl sulfate in acetic acid/dimethyl sulfoxide. Absorption was measured at 570 nm. The results were expressed as percent viability = [*A*570 (treated cells) − background]/[*A*570 (untreated cells) − background] × 100.

2.3.6. Differential scanning calorimetry (DSC)

Lipids were dispersed in MilliQ water to a concentration of 1 mg mL^{-1}. After hydration, the dispersions were vortexed, sonicated and heated above the phase transition temperature for several times. DSC measurements were performed on a microcalorimetry system (MCS DSC, MicroCal Inc., Northampton, MA). Sample and reference were degassed for at least 20 min by slow stirring under vacuum. After filling, the DSC cells were kept under 2 bar of nitrogen pressure to prevent evaporation at higher temperatures. The heating rate was 60 K h^{-1}. Samples were scanned for at least six times after being cooled down to 10 °C in order to check for reproducibility.

2.3.7. Wide angle X-ray diffraction (WAXS)

Lipids were prepared as described above for DSC experiments. Lipid concentrations of 15–20 wt% in MilliQ water were used. All samples were transferred into glass capillaries (inner diameter 1.5 mm, GLAS, Germany) and stored for 7–10 days at 4 °C before the measurements.

Wide angle X-ray scattering (WAXS) experiments were carried out at the Soft Condensed Matter beamline A2, HASYLAB, DESY (Hamburg, Germany). WAXS data were collected by a linear detector with delay line readout. The incoming beam had a wavelength of 0.15 nm, and the exposure time was 30 s. The temperature was fixed during the measurements. After each heating step, a waiting time of 5 min was used to ensure that the sample is in equilibrium. Polyethylene terephthalate was used for calibration. Positions of the Bragg peaks were converted into reciprocal spacings $s = 1/d$ with d being the real space repeat distances of the lattice planes.

2.3.8. Size measurements

The sizes of liposomes and lipoplexes were measured in distilled water by photon correlation spectroscopy on a HPPSsET (Malvern, U.K.) with sample refractive index of 1.33 and a viscosity of 0.8872 mPa s at 25 °C. Lipoplexes were prepared as for transfection experiments and measured with 2.5 μg DNA/mL sample. The *z*-average and PDI were calculated by using the automatic mode. Every sample was measured three times. Each spectroscopic run consists of 10 consecutive scans with a duration of 10 s. Results shown are the average of these three values.

2.3.9. Zeta potential measurements

Zeta potential (ζ) measurements of liposomes and lipoplexes were performed with a Zetasizer Nano ZS (Malvern, U.K.) in distilled water. Based on the Hemholtz–Smoluchowski relation, the ζ potential was automatically calculated by dispersions software 4.0 (Malvern, U.K.). Liposomes and lipoplexes, prepared as for transfection experiments and measured with 2.5 μg DNA/mL sample,

were measured with defined viscosity (0.8872 mPa s) and refractive index (1.33) at 25 °C by three runs. Results shown are the average of these three values.

2.3.10. Statistical analysis

All measurements were repeated several times ($n \geq 3$–9) and expressed as means ± standard deviation. One-way ANOVA was used in conjunction with Bonferoni's multiple comparison test to assess the statistical significance.

3. Results and discussion

3.1. Synthesis of malonic acid diamides

The synthesis of the compounds is shown in Scheme 1. The starting material was the malonic acid diethyl ester, which was converted into monoalkylated malonic acid ester **1a,b** via treatment with hexadecyl bromide or oleyl methansulfonate using published methods (Schmidt and Jankowski, 1996). This reaction allows a simple variation of the alkyl chain by using different alkyl halides or methansulfonates. The next reaction step was a selective saponification with the aim that one ester function remains preserved as a protective group for the following amide coupling. This mono-saponification was performed using described methods (Breslow et al., 1944). A second alkyl chain was introduced by coupling the alkyl malonic acid monoethyl esters **2a,b** with hexadecylamine or oleylamine to prepare the 2-alkyl malonic acid ester amides **3a**–**c**. For this reaction EEDQ[2] was used owing to the good experience made in earlier works (Heinze et al., 2010). Following, the second carboxylic acid ester group was transformed into the free acid group of **4a**–**c** by a further saponification step using potassium hydroxide as saponification agent. The received carbonic acids were coupled with tris(aminoethyl)amine building the malonic acid diamides **5a**–**c** which were already reported (Heinze et al., 2010). The described synthesis was modified by using PyBOP® instead of BOP[2] due to the cancerogenic potential described for hexamethylphosphoramide, a byproduct of the BOP coupling (Coste et al., 1990). To enlarge the cationic head group and increase the number of protonable amino groups, the proteinogenic amino acid lysine was chosen. For coupling the amino acid via amide bond to the tris(aminoethyl)amine spacer Boc-Lys(Boc)-OSu[2], as an activated Boc-protected derivative of lysine, was used. The activation of the carbonyl group as *N*-hydroxysuccinimide ester enables a racemisation-free amide coupling reaction (McDermott and Benoiton, 1973). Therefore, we can assume that the stereogenic centre in the lysine moiety is *S*-configured. First, we tried to synthesize the compounds **6a**–**c** and **7a**–**c** in one reaction by using a reaction ratio of lipid **5a**–**c** to Boc-Lys(Boc)-OSu of 1:1.5 (n/n). However, using this ratio the compounds **6b** and **6c** were isolated in a yield lower than 5% so that only the bislysine derivatives **7b** and **7c** yielded in satisfactory amounts. Because of this observation, the bislysine derivative **7a** was synthesized with a reaction ratio of 1:2 (n/n), with the aim not to waste the reactant **5a**. The monolysine derivatives **6a**–**c** could only be obtained in an adequate yield by using a reaction ratio of 1:0.5 (n/n). Due to the fact that the yield is at most 50% using the reactants **5a**–**c**, one should attempt to improve this reaction step by using a protected tris(aminoethyl)amine derivative. Finally, the cationic lipids **8a**–**c** and **9a**–**c** could be obtained by treating the Boc-protected derivatives **6a**–**c** respectively **7a**–**c** with trifluoro acetic acid. The new lipids were chemically characterized and tested with regard to their transfection efficiency.

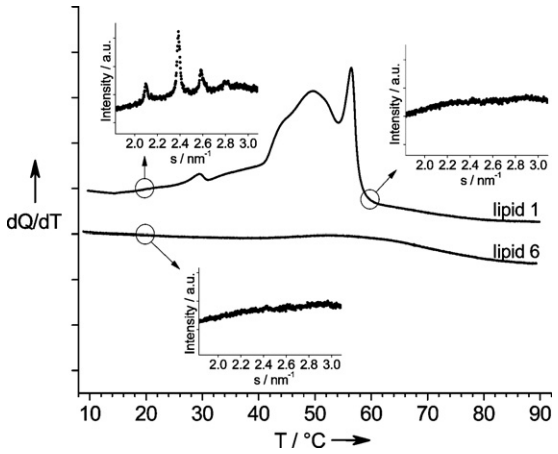

Fig. 2. Representative DSC (heat flow dQ/dT versus temperature T) and WAXS (intensity versus reciprocal spacing s) data of **lipids 1** and **6**. The WAXS patterns are taken at temperatures marked with circles in the corresponding thermograms.

3.2. In vitro transfection efficiency and cell toxicity of new malonic acid diamides

To enhance gene transfection efficiency of cationic lipids, they are usually mixed with co-lipids and used as liposomes. Most frequently, cholesterol and DOPE are used as co-lipids (Kim et al., 2004; Ma et al., 2007; Mukherjee et al., 2005). These lipids help to enable liposome formation, furthermore, they contribute to the structure and physicochemical characteristics of the lipoplexes, which are formed after incubation of cationic liposomes with DNA, resulting in an influence on the transfection efficiency (Koltover et al., 1998; Simberg et al., 2001; Zidovska et al., 2009; Zuhorn et al., 2002, 2005). Although the great influence of co-lipids for the transfection efficiency is indisputable, the mechanism of interaction is not fully understood and depends on many parameters. Currently it is not possible to predict the ideal co-lipid, therefore a screening for the optimal helper lipid for transfection experiments is necessary. DOPE and cholesterol were also used as co-lipids in the present case and mixed in different molar ratios with the tested cytofectines to find the most effective lipid/co-lipid ratio. To find the most effective N/P ratio[2] for transfection, the DNA was mixed with different amounts of these lipid mixtures. Only the data of the *in vitro* transfection tests using the lipid/co-lipid ratios respectively N/P ratios, which gave the best results, are shown. Surprisingly, **lipid 1** and **lipid 2** do not form liposomes neither with DOPE nor with cholesterol as co-lipid. Hence, no information about the *in vitro* transfection efficiency of these lipids could be obtained.

A strong self-association could be responsible for the inability of these lipids to form liposomes. Also the observation of crystalline aggregates during the liposome preparation is in agreement with such an assumption. Therefore, DSC and WAXS experiments were used to show that **lipid 1** and **lipid 2** are in a highly ordered gel state, whereas **lipids 3**, **4**, **5** and **6** are in the liquid-crystalline state at room temperature. In Fig. 2, representative DSC and WAXS data of **lipid 1** are compared with those of **lipid 6.** The other lipids are still under examination, and a detailed discussion of the thermodynamical and structural data will follow soon elsewhere.

The WAXS pattern of **lipid 1** reveals an orthorhombic chain lattice ($s_{11} = 2.38\,nm^{-1}$, $s_{02} = 2.59\,nm^{-1}$) at 20 °C. The unit cell perpendicular to the chain axis is $5.0 \times 7.7\,Å^2$ and therefore very close to the well known herringbone arrangement ($5.0 \times 7.5\,Å^2$) of hydrocarbon chains in organic crystals. The packing of the chains is extremely tight. Additionally, a Bragg peak at $s = 2.10\,nm^{-1}$ represents hydrogen bonds between the head groups with a fixed repeat distance of ~0.476 nm. The Bragg peak at $2.80\,nm^{-1}$ belongs also

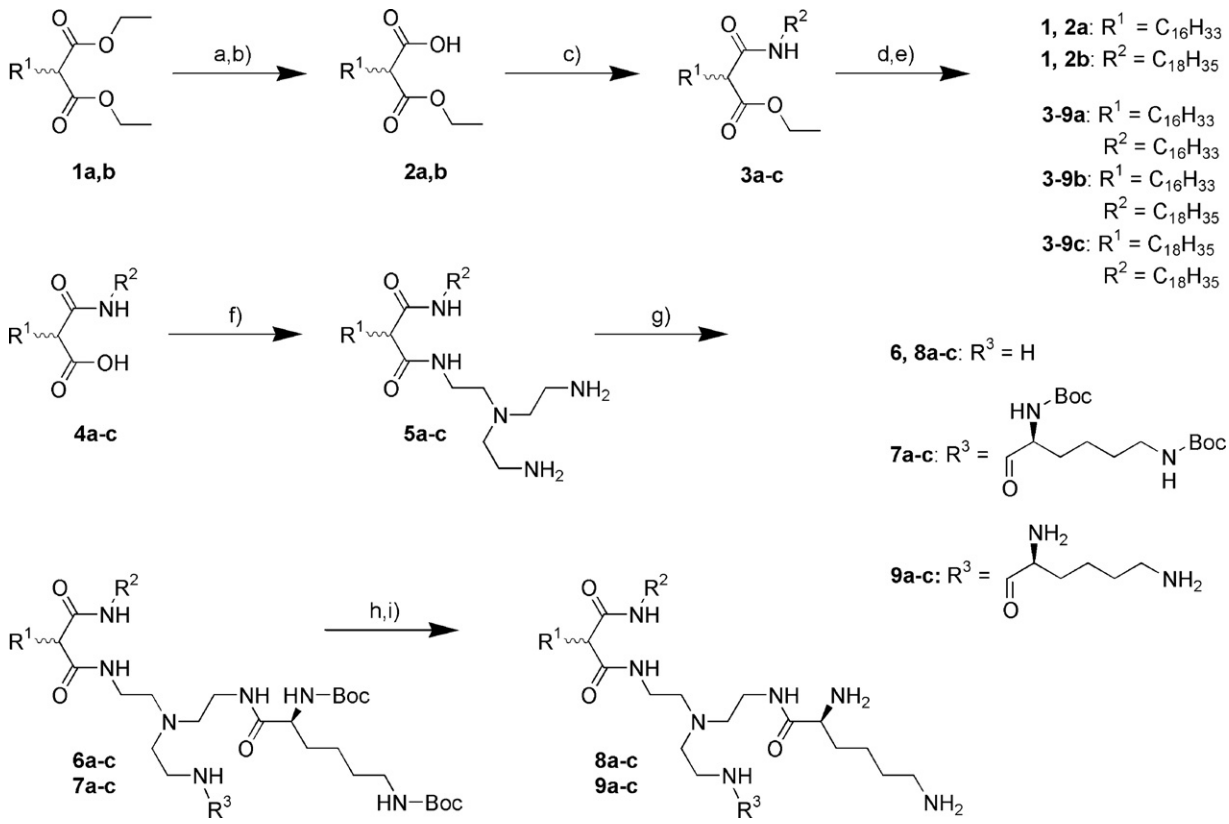

Scheme 1. Synthesis of novel cytofectines starting from alkyl malonic acid diethyl ester: (a) KOH, EtOH, rt; (b) HCl, H_2O, 0 °C; (c) R^2NH_2, EEDQ, EtOH, 50 °C; (d) KOH, EtOH, 80 °C; (e) HCl, H_2O, 0 °C; (f) $N(CH_2CH_2NH_2)_3$, TEA, PyBOP®, CH_2Cl_2, rt; (g) Boc-Lys(Boc)-OSu, TEA, CH_2Cl_2, rt; (h) TFA, CH_2Cl_2, rt; (i) NH_3 (3% m/m), $CHCl_3$.

to the proposed head group lattice, which is still under investigation. The phase formed at room temperature is therefore a sub-gel phase.

Strong attractive forces (van der Walls interactions of the lipid chains and hydrogen bonding of the head groups) will reduce the degree of hydration of the head groups. Water molecules are not able to penetrate in between the heads. The broad transition that precedes the peak at 56 °C in the DSC thermogram could be due to a stepwise breaking of the hydrogen bonds. Only afterwards, the hydrocarbon chains can melt. At 60 °C, the disappearance of all peaks in the WAXS pattern evidences the liquid-crystalline state with molten chains of **lipid 1**. The DSC scans are reversible after cooling. The poor hydration behavior due to strong hydrogen bonding networks can be a first explanation for the observation of crystalline aggregates during the liposome preparation. The homogeneous incorporation of helper lipids seems to be extremely difficult.

In contrast, **lipid 6** is already in the liquid-crystalline state at 20 °C. The WAXS patterns show no Bragg peaks, and the DSC thermogram does not show any transition peak up to high temperatures. Therefore, the chains are disordered, the molecules occupy larger areas, and the heads are fully hydrated. The homogeneous incorporation of proper helper lipids can be easily performed, and the liposomes are therefore more stable.

Fig. 3 summarizes the relative *in vitro* gene delivery efficiencies of **lipid 6** mixed with the co-lipid DOPE in a lipid/co-lipid ratio of 2:1 (n/n) after 48 h in A549 cells using different N/P ratios. The figure shows increasing transfection efficiency by increasing the N/P ratio. Using a N/P ratio of 3.33, the observed transfection efficiency surpasses those of the references LipofectAmine™ and SuperFect™. These results are statistical significant (*). Furthermore, in Fig. 3 **lipid 6** is compared with **lipid 3** which contains the same lipophilic molecule part but only one lysine moiety attached to the tris(aminoethyl)amine spacer. As shown, **lipid 6** achieves a statistically significant higher transfection efficiency (*) than **lipid 3**. **Lipid 3** is comparable with the reference substances LipofectAmine™ and SuperFect™ with regard to the transfection efficiencies. These results show that the introduction of a second lysine moiety in the head group area of the malonic acid diamides increases the transfection efficiency in A549 cells. The results of the MTT based cytotoxicity experiments of **lipid 6** in A549 cells are shown in Fig. 4.

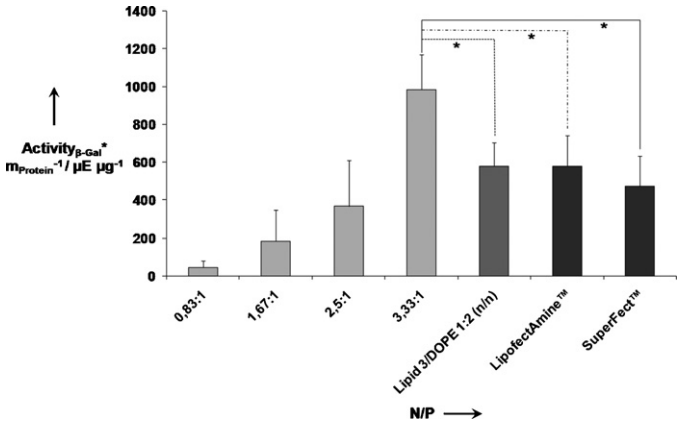

Fig. 3. *In vitro* transfection efficacies of **lipid 6** in A549 cells using DOPE as co-lipid (at lipid/DOPE molar ratio of 2:1). Micro units of β-galactosidase related to cell protein concentration were plotted against the varying N/P ratios. The transfection efficiencies of the liposome samples were compared to those of **lipid 3**/DOPE 1:2 (n/n) with a N/P ratio of 4 and of the commercially available LipofectAmine™ and SuperFect™. The transfection values shown are the average of at least three experiments carried out on three different days. Statistical analyses were carried out with $p < 0.05$, one-way ANOVA, and Bonferoni's multiple comparison tests (*).

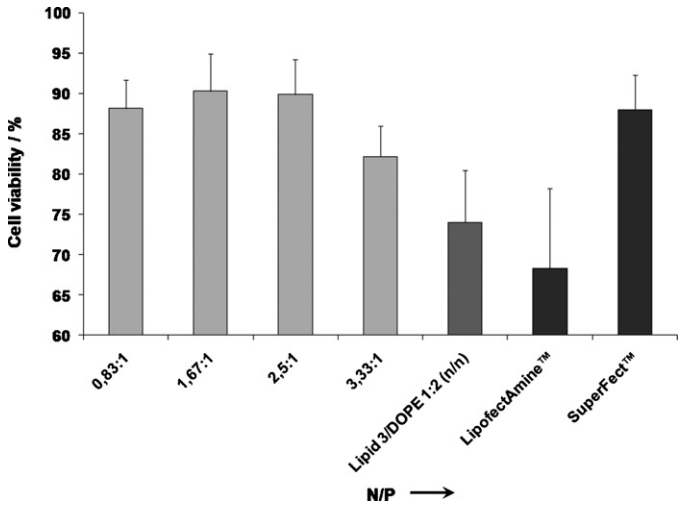

Fig. 4. MTT-based cellular cytotoxicity of **lipid 6** using DOPE as co-lipid (at a lipid/co-lipid molar ratio of 2:1) in A549 cells. The percent cell viability was plotted against the varying N/P ratios. The results are compared to those of **lipid 3**/DOPE 1:2 (n/n) with a N/P ratio of 4, LipofectAmine™, and SuperFect™. The experiments were performed as described in the text. The cytotoxicity values shown are the average of at least three experiments carried out on different days.

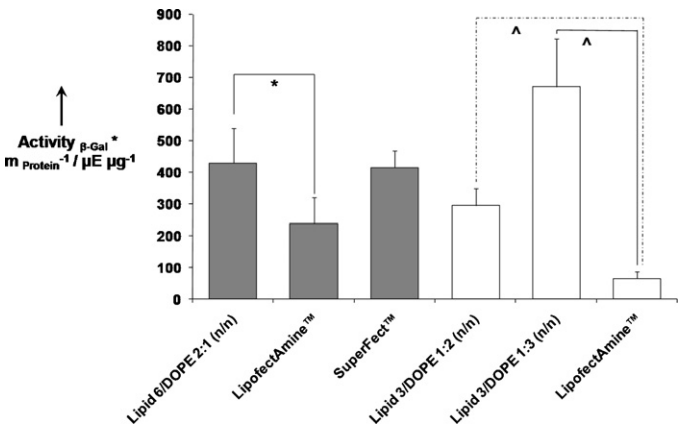

Fig. 6. *In vitro* transfection efficacies of **lipid 6** and **lipid 3** in LLC PK1 (gray) and A549 (white) cells in the presence of serum compared with LipofectAmine™ and SuperFect™. Concentration of FBS was adjusted to 10% at the outset and kept for 48 h. N/P ratios: **lipid 6**, 3.33:1; **lipid 3**, 4:1. The transfection values shown are the average of leastwise three experiments carried out on three different days. Statistical analyses were carried out with $p < 0.05$, one-way ANOVA, and Bonferoni's multiple comparison tests (*, ^).

It can be seen that increasing lipid concentration (higher N/P ratio) results in decreasing cell viability. Nevertheless, the observed viability in all tested N/P ratios is higher than that observed for LipofectAmine™ and **lipid 3**/DOPE 1:2 (n:n).

Fig. 5 summarizes the results of *in vitro* gene delivery of **lipid 4**, **lipid 5**, and **lipid 6** in LLC PK1 cells after 48 h. The graph shows the most efficient N/P ratios for the used lipids in combination with either cholesterol or DOPE as co-lipid. The three tested lipids have the same hydrophilic protonable head group but differ in the length (two CH_2-units) and the saturation degree of the alkyl chains. It can be seen, that an increase of the number of unsaturated alkyl chains results in higher transfection efficacies, regardless of using DOPE or cholesterol as co-lipid. The fact that an increase of the alkyl chain fluidity, e.g. by using unsaturated chains, leads to increasing transfection efficacies has been already observed in earlier works in the research group (Heinze et al., 2010) and is also described in the literature (Bennett et al., 1998; Felgner et al., 1994; Spector and Schnur, 1997). Furthermore, it can be seen that DOPE is the more effective co-lipid compared to cholesterol (except **lipid 4**). This observation is in contrast to results achieved earlier with malonic acid diamides containing a smaller head group, which often obtained

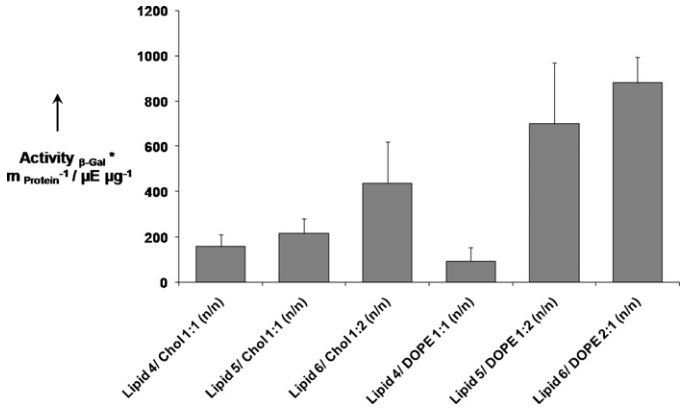

Fig. 5. *In vitro* transfection efficacies of **lipid 4**, **lipid 5**, and **lipid 6** in LLC PK1 cells. N/P ratios: **lipid 4**, 2.5:1; **lipid 5**, 1.67:1 (Chol), 3.33:1 (DOPE); and **lipid 6**, 2.5:1 (Chol), 1.67:1 (DOPE). The transfection values shown are the average of leastwise three experiments carried out on three different days.

better transfection results with cholesterol as co-lipid (Heinze et al., 2010). Since the polar head group of DOPE is larger in comparison to cholesterol, stronger interactions with the large head group of the tested malonic acid amides might be responsible for this effect. In contrast to this, **lipid 4** which contains two hexadecyl chains shows better transfection efficacy with cholesterol. It is known that cholesterol has a fluidizing effect on lipid bilayers by disturbing the packing of the alkyl chains (Oldfield and Chapman, 1972), what seems to be the most reasonable explanation for this observation. However, precise explanations cannot be made without further physicochemical investigations of the lipoplexes of malonic acid diamides with co-lipids. Interestingly, **Lipid 6**/DOPE 2:1 (n/n) shows a statistically significant better transfection efficacy than LipofectAmine™ (data not shown) also observed in A549 cells (see Fig. 3).

3.3. *In vitro transfection in presence of serum*

With the aim to realize *in vivo* application it is necessary to use lipids forming lipoplexes which are stable in the presence of serum. To get first evidence for the serum compatibility of the selected lipids, cells were incubated with the lipoplexes in the presence of 10% FBS for 48 h. Admittedly, total protein concentration of human serum, which is between 66 and 83 $g\,l^{-1}$ (Schaller et al., 2008), is just reached with a level of 60%, but first information about serum compatibility of the used lipoplexes can still be obtained.

Fig. 6 summarizes the transfection results achieved with **lipid 6** and **lipid 3** in LLC PK1 cells (gray) and A549 cells (white) in presence of serum compared with LipofectAmine™ or SuperFect™. First it should be mentioned that a decrease of the gene transfer was observed for nearly all tested lipids compared to gene transfer without serum over a period of 4 h from the beginning of the incubation. But the decrease was not as strong as observed for LipofectAmine™ which shows very low transfection efficacy in A549 cells when serum was added from the beginning. All lipids are significantly better than LipofectAmine™ with regard to transfection efficacy (*, ^). In A549 cells, **lipid 3** surpasses LipofectAmine™ extensively. Surprisingly, the mixture **lipid 3**/DOPE 1:3 (n/n) with a N/P ratio of 4 shows better transfection efficacies with 10% FBS used from the beginning of the incubation compared with a 4 h serum free interval at the beginning (data not shown).

Table 1
Size measurements (*z*-ave. = *z*-average, PDI values), and ζ potentials of **lipid 3**, **lipid 4**, **lipid 5**, **lipid 6**, and LipofectAmine™ using DOPE and cholesterol (Chol.) as co-lipid (at different lipid/co-lipid molar ratios). The results are given for the pure liposomes and the corresponding lipoplexes. The given *z*-average diameters, PDI values, and ζ potentials were determined by three runs.

	Liposomes			Lipoplexes		
	z-Ave.±s (nm)	PDI ± v	ζ ± s (mV)	*z*-Ave.±s (nm)	PDI ± v	ζ ± s (mV)
Lipid 3/DOPE 1:2 (n/n) N/P 4:1	68 ± 1	0.33 ± 6%	32.1 ± 2.5	109 ± 1	0.16 ± 10%	23.5 ± 0.86
Lipid 3/DOPE 1:3 (n/n) N/P 4:1	103 ± 3	0.25 ± 8%	28.6 ± 2.7	184 ± 1	0.18 ± 1%	22.5 ± 1.66
Lipid 4/DOPE 1:1 (n/n) N/P 2.5:1	232 ± 6	0.46 ± 5%	19.5 ± 5.7	93 ± 1	0.35 ± 1%	9.6 ± 0.51
Lipid 4/Chol. 1:1 (n/n) N/P 2.5:1	85 ± 5	0.76 ± 3%	38.3 ± 2.8	244 ± 4	0.71 ± 4%	8.1 ± 1.31
Lipid 5/DOPE1:2 (n/n) N/P 3.33:1	623 ± 67	0.72 ± 25%	30.6 ± 1.7	853 ± 29	0.07 ± 45%	8.2 ± 1.56
Lipid 5/Chol. 1:1 (n/n) N/P 1.67:1	91 ± 1	0.22 ± 5%	47.6 ± 2.2	103 ± 2	0.23 ± 7%	8.9 ± 0.88
Lipid 6/DOPE2:1 (n/n) N/P 1.67:1	1592 ± 98	0.16 ± 42%	39.3 ± 1.9	450 ± 1	0.31 ± 1%	6.3 ± 0.50
Lipid 6/DOPE2:1 (n/n) N/P 3.33:1	1592 ± 98	0.16 ± 42%	39.3 ± 1.9	1415 ± 53	0.32 ± 29%	14.5 ± 2.17
Lipid 6/Chol. 1:2 (n/n) N/P 2.5:1	142 ± 6	0.37 ± 17%	38.7 ± 3.2	992 ± 33	0.22 ± 12%	6.6 ± 0.71
LipofectAmine™ N/P 3:1	154 ± 10	0.54 ± 25%	48.4 ± 3.2	120 ± 1	0.20 ± 7%	30.7 ± 0.9
LipofectAmine™ N/P 9:1	154 ± 10	0.54 ± 25%	48.4 ± 3.2	107 ± 1	0.20 ± 1%	39.3 ± 4.2

3.4. Size measurements of liposomes and lipoplexes

Table 1 summarizes the results of size measurements of liposomes and lipoplexes. The polydispersity index (PDI) is also shown. The PCS measurements of the cationic liposomes respectively lipoplexes show that the particle sizes differ very much. Since the liposome size strongly depends on the method of liposome preparation, and furthermore, the liposome structures change during lipoplex formation, we will focus on lipoplex sizes in the following part. Lipoplexes from 100 nm to nearly 1500 nm (comparing the different lipids at different lipid/co-lipid and N/P ratios) have been observed. The main question was whether a correlation between particle size and transfection efficiency exists.

Fig. 7 shows the dependence of the particle size on the N/P ratio in case of **lipid 6**/DOPE 2:1 (n/n) lipoplexes. Decreasing N/P ratio leads to a decrease of the particle size, a phenomenon that has been described in literature earlier (Eastman et al., 1997). Comparing the particle size (Fig. 7) with the transfection efficiencies (Fig. 3) shows that larger lipoplexes are more effective in gene transfer, an observation which was made by other researches too (Sakurai et al., 2000). Zuhorn proposed that the particle size may reflect the structural instability needed for perturbing intracellular membrane barriers to allow cytosolic escape of DNA resulting in higher transfection efficiency (Shi et al., 2002; Zuhorn et al., 2007). Other arguments for the observed higher transfection efficiency of larger lipoplexes are the dependence of endocytosis pathways from particle sizes (Zuhorn et al., 2007), and a better sedimentation of larger particles during lipoplex incubation of cells *in vitro* (Ma et al., 2007). Furthermore, this figure illustrates the drastic size change by mixing liposomes with DNA. Starting from liposomes with a *z*-average of 1592 nm, the decrease of the N/P ratio decreases continuously the lipoplex size to values below 400 nm. In contrast, Table 1 shows that in most cases the lipoplexes have larger diameters compared to the corresponding liposomes.

Comparing the transfection results (Fig. 5) with lipoplex sizes shows a tendency, that larger lipoplexes are more efficient in gene transfer. But it is difficult to make clear correlations between particle sizes and transfection efficacy because the lipoplexes differ in the cationic lipid, the type and amount of co-lipid, and the N/P ratio. These three factors influence either transfection efficiency or particle size. It is an interesting question whether the particle size influences directly the transfection efficiency or can be taken only as an indicator, resulting from other factors enhancing gene transfer directly. The influence of particle size is still controversially discussed (Ma et al., 2007; Zuhorn et al., 2007).

The comparison of Fig. 6 with Table 1 is interesting. The most effective lipid–DNA mixture of **lipid 6**/DOPE 2:1 (n/n) N/P 3.33:1 in LLC PK1 cells forms very large lipoplexes (1415 nm) compared to the two effective mixtures of **lipid 3** in A549 cells which form only very small particles (109 nm and 184 nm). The results of **lipid 3** contradict statements made in literature earlier (Ma et al., 2007; Turek et al., 2000), proposing that lipoplexes of less than 250 nm in size show efficient transfection only in the absence of serum. As mentioned above, **lipid 3**/DOPE 1:3 (n/n) with N/P ratio of 4 shows better transfection results in presence of serum, compared with serum free tests. The measurements in serum were made with regard of a possible application *in vivo*. For successful *in vivo* gene transfer, particles should have a size less than 150 nm, because larger ones are quickly cleared from blood (Kayser and Kiderlen, 2004; Li and Szoka, 2007). Therefore, the particle sizes of **lipid 3** are preferential for *in vivo* application, whereas the size of **lipid 6**/DOPE 2:1 (n/n) N/P 3.33:1 only allows *ex vivo* application. But, one has to take into account that the size measurements were carried out under idealized conditions with water as medium. Salt containing medium or serum could influence the particle size drastically. Because of this, the measured *z*-averages must not reflect the true particle sizes during transfection experiments. We tried to investigate the particle size in serum, but because of the serum proteins this is not possible by PCS.

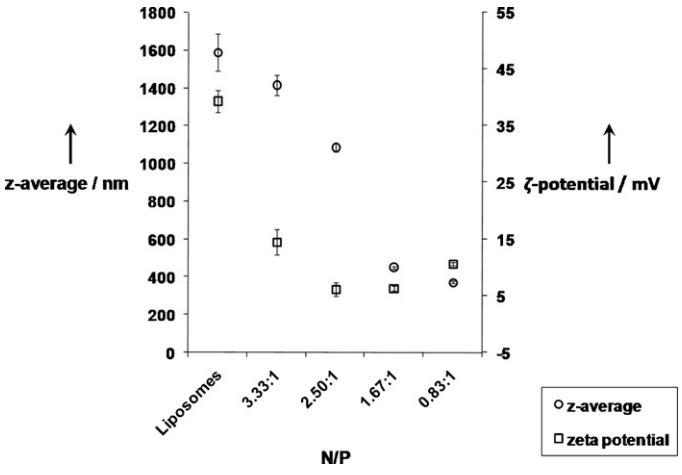

Fig. 7. Photon correlation spectroscopy analyses and ζ potential measurements of liposomes and lipoplex mixtures of **lipid 6** using DOPE as co-lipid (at lipid/DOPE molar ratio of 2:1). First *y*-axis (circles): changes of liposome and lipoplex size as a function of decreasing lipid concentration (concentration of DNA = 2.5 μg/mL). The average diameters of liposomes and lipoplexes were determined by three spectroscopic runs comprising ten consecutive scans, each of 10 s duration. Second *y*-axis (squares): changes of ζ potentials of liposomes and lipoplexes as a function of decreasing lipid concentration (concentration of DNA = 2.5 μg/mL). The ζ potentials of liposomes and lipoplex particles were determined by three runs.

3.5. Zeta potential measurements of liposomes and lipoplexes

Both liposomes and lipoplexes were investigated with regard to their surface charge by ζ potential measurements in water. This allows to the direct comparison with the PCS measurements. The obtained ζ potentials are shown in Table 1. The charges measured for the liposomes are in the range between +20 mV and +50 mV depending on the co-lipid and the lipid/co-lipid ratio (Perrie and Gregoriadis, 2000). Also the potential of LipofectAmine™ (+48.4 mV) is in this range. Comparing the ζ potentials with the gene transfer efficiency, no direct correlation could be observed. For example, the efficient lipid mixture (**lipid 6**/DOPE 2:1 (n/n)) and the ineffective mixture (**lipid 4**/cholesterol 1:1 (n/n)) show nearly the same ζ potential (Table 1 and Fig. 5).

For all lipid mixtures used, the ζ potential decreases after addition of DNA (Table 1). This shows that DNA successfully couples to the liposomes to form the lipoplexes. Interestingly, the ζ potential of all lipoplexes investigated is still positive showing that the DNA coupling does not lead to a charge reversal. There are different theories in literature explaining the positive ζ potential of lipoplexes, either by an entrapment of DNA by the surrounding cationic lipids or a partial adsorption of DNA at the surface (Eastman et al., 1997; Ma et al., 2007; Mevel et al., 2008). Further investigations of the lipoplex morphology are needed to get a clear answer.

Fig. 7 shows the change of the ζ potential for the **lipid 6**/DOPE 2:1 (n/n) mixture in dependence of the N/P ratio. A decrease of the positive charge after mixing the liposomes with DNA can be seen. It seems that the decrease of the ζ potential levels off around +7 mV below a N/P ratio of 2.5:1. Again, comparing the ζ potential (Fig. 7) with the transfection efficiency (Fig. 3), no clear correlation can be observed.

The charges of the other lipoplexes formed with **lipid 4**, **lipid 5** and **lipid 6** (by varying N/P ratios and co-lipids) are all in the range of +6 mV to +15 mV, and do also not correlate with the gene transfer efficiency (comparing Table 1 and Fig. 5). Only **lipid 3** and LipofectAmine™ show in their lipoplexes higher positive values of the ζ potential. In the case of **lipid 3**, a smaller decrease of the ζ potential after lipoplex formation has been observed (compared with the values for **lipids 4–6**). This is maybe a hint for efficient DNA entrapment in multilamellar lipoplex structures (Ma et al., 2007) explaining the good transfection results in serum. However, the high N/P ratio of 4 can also explain this observation, because LipofectAmine™ shows high charge values at high N/P ratios too (Table 1). Interestingly, the values measured for the lipoplexes of **lipid 3**/DOPE with an N/P ratio of 4 at different lipid/co-lipid ratios (1:2 or 1:3) are nearly the same, which supports the idea of good DNA entrapment into the lipoplex structure. But, as mentioned above further structural investigations are need.

4. Conclusions

By designing new lipids for non-viral gene delivery it is important to investigate structure–activity relationships to expedite the development of cytofectines. This work extends the effort to find such structure–activity relationships for the new class of cytofectines with malonic acid diamide backbone by enlarging the head group region. In agreement with the results of earlier works we found that the insertion of at least one unsaturated alkyl chain leads to higher transfection efficacies. Furthermore, in the case of **lipid 3** and **lipid 6** tested in A549 cells, it was shown that an enlargement of the cationic head group, by coupling with two lysine molecules instead of only one, results in an enhancement of the transfection efficiency. Unfortunately, this observation could not be supported by using the other malonic acid diamides which contain one or two saturated alkyl chains in the lipophilic molecule part, because of the inability of **lipid 1** and **lipid 2** to form liposomes.

Surprisingly, predominantly DOPE turns out to be the more effective co-lipid in contrast to the observation made for the other malonic acid diamides, which contain a smaller head group. For them cholesterol was found to be more efficacious. In summary, a series of new cationic malonic acid diamides was synthesized and chemically characterized. The testing of these new compounds in cell culture with regard to transfection efficacy and cytotoxicity shows that they are able to transfer genetic material with low toxicity. In some cases, the tested lipids were considerably better than the references LipofectAmine™ and SuperFect™. **Lipid 6** has the highest transfection potential of the six new lipids in both cell lines.

Finally, **lipid 3** and **lipid 6** show promising transfection results in the presence of serum. Although in most cases a decreasing of the transfection efficacies was observed in serum in comparison with serum free tests, these lipids show significantly better results than LipofectAmine™. Surprisingly, **lipid 3**/DOPE 1:3 (n/n) with a N/P ratio of 4 shows even better transfection results in presence of serum compared to tests using a serum free interval at the beginning.

First DSC and WAXS experiments show a clear correlation between the phase transition parameters as well as phase structures and the ability of the new lipids to form stable liposomes as a precondition for successful transfection. The investigations of the particle size and ζ potential gives interesting results for first discussion, but do not generate clear correlations between these parameters and the transfection efficiency. Therefore, further investigations are need to find the most important parameters for such a correlation, which would make the time intensive and costly cellular transfection screening experiments unnecessary.

Acknowledgments

We thank the Max Planck Institute of Colloids and Interfaces Potsdam for financial support, and HASYLAB at DESY, Hamburg, Germany, for beamtime and excellent support. Furthermore, the authors wish to thank Dr. Christian Ihling and Prof. Dr. Andrea Sinz (Institute of Pharmacy, Martin-Luther-University, Halle (Saale), Germany) for the high resolution mass spectrometry analyses.

References

Bennett, C.F., Mirejovsky, D., Crooke, R.M., Tsai, Y.J., Sridkar, C.N., Wheeler, C.J., Felgner, P.L., 1998. Structural requirements for cationic lipid mediated phosphorothioate oligonucleotides delivery to cells in culture. J. Drug Target. 5, 149–162.
Bhattacharya, S., Bajaj, A., 2009. Advances in gene delivery through molecular design of cationic lipids. Chem. Commun., 4632–4656.
Breslow, D.S., Baumgarten, E., Hauser, C.R., 1944. A new synthesis of β-keto esters of the type $RCOCH_2COOC_2H_5$. J. Am. Chem. Soc. 66, 1286–1288.
Coste, J., Le-Nguyen, R., Castro, B., 1990. PyBOP®: a new peptide coupling reagent devoid of toxic by-product. Tetrahedron Lett. 31, 205–208.
Eastman, S.J., Siegel, C., Tousignant, J., Smith, A.E., Cheng, S.H., Scheule, R.K., 1997. Biophysical characterisation of cationic lipid: DNA complexes. Biochim. Biophys. Acta 1325, 41–62.
El-Aneed, A., 2004. An overview of current delivery systems in cancer gene therapy. J. Control. Rel. 94, 1–14.
Felgner, J.H., Kumar, R., Sridhar, C.N., Wheeler, C.J., Tsai, Y.J., Border, R., Ramsey, P., Martin, M., Felgner, P.L., 1994. Enhanced gene delivery and mechanism studies with a novel series of cationic lipid formulations. J. Biol. Chem. 269, 2550–2561.
Heinze, M., Brezesinski, G., Dobner, B., Langner, A., 2010. Novel cationic lipids based on malonic acid amides backbone: transfection efficacy and cell toxicity properties. Bioconjugate Chem. 21, 696–708.
Hyde, S.C., Southern, K.W., Gileadi, U., Fitzjohn, E.M., Mofford, K.A., Waddell, B.E., Gooi, H.C., Goddard, C.A., Hannavy, K., Smyth, S.E., Egan, J.J., Sorgi, F.L., Huang, L., Cuthbert, A.W., Evans, M.J., Colledge, W.H., Higgins, C.F., Webb, A.K., Gill, D.R., 2000. Repeat administration of DNA/liposomes to the nasal epithelium of patients with cystic fibrosis. Gene Ther. 7, 1156–1165.
Kay, M.A., Glorioso, J.C., Naldini, L., 2001. Viral vectors for gene therapy: the art of turning infectious agents into vehicles of therapeutics. Nat. Med. 7, 33–40.
Kayser, O., Kiderlen, A.F., 2004. Non viral gene delivery systems. In: Pharmaceutical Biotechnology. Wiley-VCH, Weinheim.
Kim, H.S., Moon, J., Kim, K.S., Choi, M.M., Lee, J.E., Heo, Y., Cho, D.H., Jang, D.O., Park, Y.S., 2004. Gene-transferring efficiencies of novel diamino cationic lipids with varied hydrocarbon chains. Bioconjugate Chem. 15, 1095–1101.

Koltover, I., Salditt, T., Radler, J.O., Safinya, C.R., 1998. An inverted hexagonal phase of cationic liposome-DNA complexes related to DNA release and delivery. Science 281, 78–81.
Li, W., Szoka Jr., F.C., 2007. Lipid-based nanoparticles for nucleic acid delivery. Pharm. Res. 24, 438–449.
Luger, K., Mäder, A.W., Richmond, R.K., Sargent, D.F., Richmond, T.J., 1997. Crystal structure of the nucleosome core particle at 2.8 Å resolution. Nature 389, 251–260.
Lv, H., Zhang, S., Wang, B., Cui, S., Yan, J., 2006. Toxicity of cationic lipids and cationic polymers in gene delivery. J. Control. Rel. 114, 100–109.
Ma, B., Zhang, S., Jiang, H., Zhao, B., Lv, H., 2007. Lipoplex morphologies and their influences on transfection efficiency in gene delivery. J. Control. Rel. 123, 184–194.
McDermott, J.R., Benoiton, N.L., 1973. *N*-Methylamino acids in peptide synthesis. IV. Racemization and yields in peptide-bond formation. Can. J. Chem. 51, 2562–2570.
Mevel, M., Breuzard, G., Yaouanc, J.J., Clement, J.C., Lehn, P., Pichon, C., Jaffres, P.A., Midoux, M., 2008. Synthesis and transfection activity of new cationic phosphoramidate lipids: high efficiency of an imidazolium derivative. ChemBioChem 9, 1462–1471.
Mintzer, M.A., Simanek, E.E., 2009. Nonviral vectors for gene delivery. Chem. Rev. 109, 259–302.
Mosmann, T., 1983. Rapid colorimetric assay for cellular growth and survival: application to proliferation and cytotoxicity assays. J. Immunol. Methods 65, 55–63.
Mukherjee, K., Sen, J., Chaudhuri, A., 2005. Common co-lipids, in synergy, impart high gene transfer properties to transfection-incompetent cationic lipids. FEBS Lett. 579, 1291–1300.
Nazari, R., Jashi, S., 2009. Recent developments in the use of adenoviruses and immunotoxins in cancer gene therapy. Curr. Gene Ther. 9, 20–25.
Noone, P.G., Hohneker, K.W., Zhou, Z., Johnson, L.G., Foy, C., Gipson, C., Jones, K., Noah, T.L., Leigh, M.W., Schwartzbach, C., Efthimiou, J., Pearlman, R., Boucher, R.C., Knowles, M.R., 2000. Safety and biological efficacy of a lipid–CFTR complex for gene transfer in the nasal epithelium of adult patients with cystic fibrosis. Mol. Ther. 1, 105–114.
Oldfield, E., Chapman, D., 1972. Molecular dynamics of cerebroside-cholesterol and sphingomyelin—cholesterol interactions: implications for myelin membrane structure. FEBS Lett. 21, 303–306.
Park, T.G., Jeong, J.H., Kim, S.W., 2006. Current status of polymeric gene delivery systems. Adv. Drug Deliv. Rev. 58, 467–486.
Perrie, Y., Gregoriadis, G., 2000. Liposome-entrapped plasmid DNA: characterisation studies. Biochim. Biophys. Acta 1475, 125–132.
Quiagen® Plasmid Purification Handbook, 2011, www.kirschner.med.harvard.edu/files/protocols/QIAGEN_QIAGENPlasmidPurification_EN.pdf.
Rosenberg, I.M., 1996. Protein Analysis and Purification: Benchtop Techniques. Birkenhäuser, Boston. 0-8176-3717-6.
Sakurai, F., Inoue, R., Nishino, Y., Okuda, A., Matsumoto, O., Taga, T., Yamashita, F., Takakura, Y., Hashida, M., 2000. Effect of DNA/liposome mixing ratio on the physicochemical characteristics, cellular uptake and intracellular trafficking of plasmid DNA/cationic liposome complexes and subsequent gene expression. J. Control. Rel. 66, 255–269.
Schaller, J., Gerber, S., Kaempfer, U., Lejon, S., Trachsel, C., 2008. Human Blood Plasma Proteins. John Wiley & Sons Ltd., Chichester-West Sussex, p. 17.
Schmidt, R.R., Jankowski, K., 1996. New types of nonionic surfactants with sugar head groups. Liebigs Ann., 867–879.
Seow, Y., Wood, M.Y., 2009. Biological gene delivery vehicles: beyond viral vectors. Mol. Ther. 17, 767–777.
Shi, F., Wasungu, L., Nomden, A., Stuart, M.C.A., Polushki, E., Engberts, J.B.F.N., Hoekstra, D., 2002. Interference of poly(ethylene glycol)-lipid analogues with cationic lipid-mediated delivery of oligonucleotides; role of lipid exchangeability and non-lamellar transitions. Biochem. J. 366, 333–341.
Simberg, D., Danino, D., Talmon, Y., Minsky, A., Ferrari, M.E., Wheeler, C.J., Barenholz, Y., 2001. Lipids and lipoproteins. J. Biol. Chem. 276, 47453–47459.
Spector, M.S., Schnur, J.M., 1997. DNA ordering on a lipid membrane. Science 275, 791–792.
Turek, J., Dubertret, C., Jaslin, G., Antonakis, K., Scherman, D., Pitard, B., 2000. Formulations which increase the size of lipoplexes prevent serum associated inhibition of transfection. J. Gene Med. 2, 32–40.
Young, Z.R., Wang, H.F., Zhao, J., Peng, Y.Y., Wang, J., Guinn, B.A., Huang, L.Q., 2007. Recent developments in the use of adenoviruses and immunotoxins in cancer gene therapy. Cancer Gene Ther. 14, 599–615.
Zhang, J., Jia, D., Olson, B.E., Campbell, A.G., Thule, P.M., 2009. Hepatic insulin gene therapy diminishes liver glycogen despite insulin responsive transcriptional effects in diabetic CD-1 mice. J. Gene Med. 11, 588–597.
Zidovska, A., Evans, H.M., Ahmad, A., Ewert, K.K., Safinya, C.R., 2009. The role of cholesterol and structurally related molecules in enhancing transfection of cationic liposome–DNA complexes. J. Phys. Chem. B 113, 5208–5216.
Zuhorn, I.S., Oberle, V., Visser, W.H., Engberts, J.B., Bakowsky, U., Polushkin, E., Hoekstra, D., 2002. Phase behavior of cationic amphiphiles and their mixtures with helper lipid influences lipoplex shape, DNA translocation, and transfection efficiency. Biophys. J. 83, 2096–2108.
Zuhorn, I.S., Bakowsky, U., Polushkin, E., Visser, W.H., Stuart, M.C., Engberts, J.B., Hoekstra, D., 2005. Nonbilayer phase of lipoplex–membrane mixture determines endosomal escape of genetic cargo and transfection efficiency. Mol. Ther. 11, 801–810.
Zuhorn, I.S., Engberts, J.B.F.N., Hoekstra, D., 2007. Gene delivery by cationic lipid vectors: overcoming cellular barriers. Eur. Biophys. J. 36, 349–362.